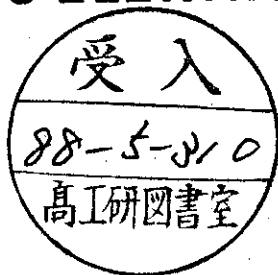


DESY 88-036
March 1988



ON THE PERIODIC ORBITS OF A STRONGLY CHAOTIC SYSTEM

by

R. Aurich, F. Steiner

II. Institut für Theoretische Physik, Universität Hamburg

ISSN 0418-9833

NOTKESTRASSE 85 · 2 HAMBURG 52

DESY behält sich alle Rechte für den Fall der Schutzrechtserteilung und für die wirtschaftliche Verwertung der in diesem Bericht enthaltenen Informationen vor.

DESY reserves all rights for commercial use of information included in this report, especially in case of filing application for or grant of patents.

**To be sure that your preprints are promptly included in the
HIGH ENERGY PHYSICS INDEX ,
send them to the following address (if possible by air mail) :**

**DESY
Bibliothek
Notkestrasse 85
2 Hamburg 52
Germany**

On the Periodic Orbits of a Strongly Chaotic System

by

R.Aurich ¹ and F.Steiner

II.Institut für Theoretische Physik , Universität Hamburg
Luruper Chaussee 149 , 2000 Hamburg 50
Federal Republic of Germany

Abstract

A point particle sliding freely on a two-dimensional surface of constant negative curvature (Hadamard - Gutzwiller model) exemplifies the simplest chaotic Hamiltonian system. Exploiting the close connection between hyperbolic geometry and the group $SU(1,1)/\{\pm 1\}$, we construct an algorithm (symbolic dynamics), which generates the periodic orbits of the system. For the simplest compact Riemann surface having as its fundamental group the "octagon group", we present an enumeration of more than 2 million periodic orbits. For the length of the n th primitive periodic orbit we find a simple expression in terms of algebraic numbers of the form $m + \sqrt{2}n$ ($m, n \in \mathbf{N}$ are governed by a particular Beatty sequence), which reveals a strange arithmetical structure of chaos. Knowledge of the length spectrum is crucial for quantization via the Selberg trace formula (periodic orbit theory), which in turn is expected to unravel the mystery of quantum chaos.

¹Supported by Deutsche Forschungsgemeinschaft under Contract No. DFG-Ste 241/4-1

I Introduction

In this paper we are presenting for the first time a detailed description of the spectrum of periodic orbits (closed geodesics) for the special case of a compact Riemann surface of genus $g = 2$. This is a surface of constant negative Gaussian curvature, $K = -1$ in appropriate units, which can be considered topologically as a double doughnut. Such surfaces are currently under intensive investigation [1], because they yield the most chaotic models of Hamiltonian systems with a few degrees of freedom. In 1898 this point of view had already been stressed by Hadamard who investigated the free motion of a mass point on such a surface. But now physicists are interested in the connection between classical chaos and its counterpart in quantum mechanics, which remains a mystery until now. There are some hints that the eigenvalue spectrum of the quantum mechanical system displays some unique statistical properties [2], if the classical counterpart is chaotic. The most promising way - as emphasized by Gutzwiller [3]- is to employ the Selberg trace formula [4,5,6], which yields a kind of duality relation between the lengths of periodic orbits of the classical system and the eigenvalues of the quantum mechanical system. Until now a direct use of this remarkable formula was impossible, because of lack of knowledge of the classical periodic orbits. In this paper we describe the properties of the length spectrum for the special case of genus $g = 2$. The application of the Selberg trace formula using this length spectrum as an input will be published in a subsequent paper.

The classical dynamics on the pseudosphere, the whole surface of constant negative curvature, can be described conveniently by one of the models which map the infinitely extended pseudosphere on a special domain of the complex plane. We use the so-called Poincaré disc, where the special domain is the interior of the unit circle, i.e. each point of the pseudosphere is mapped into the unit circle on the complex plane. There one has the metric tensor of hyperbolic geometry ($i, j = 1, 2$)

$$g_{ij} = \frac{4}{(1 - x_1^2 - x_2^2)^2} \delta_{ij} \quad (1)$$

with $z = x_1 + ix_2$ and $x_1^2 + x_2^2 < 1$. The classical motion of a particle of mass m sliding freely on a surface M of constant negative curvature is governed by the Lagrangian

$$L = \frac{m}{2} g_{ij} \frac{dx^i}{dt} \frac{dx^j}{dt} \quad (2)$$

and takes place along euclidean circles (geodesics) intersecting perpendicularly the unit circle. The classical Hamiltonian is given by

$$H = \frac{1}{2m} p_i g^{ij} p_j \quad (3)$$

where $p_i = m g_{ij} \frac{dx^j}{dt}$ and g^{ij} is the inverse of g_{ij} . (We call the dynamical system defined by (2) and (3) the Hadamard-Gutzwiller model.)

The energy $E = L = H$ is the only constant of motion, and the dynamics is the geodesic flow on M ,

$$ds = \sqrt{g_{ij} dx^i dx^j} = \sqrt{\frac{2E}{m}} dt \quad .$$

There are no invariant tori in phase space, the system has very sensitive dependence on initial conditions, and almost all orbits are dense [7]. The system has the Anosov property [8]: neighbouring trajectories diverge with time at the rate $e^{\omega t}$, i.e. the trajectories are unstable, a typical property of chaos. From Jacobi's equation for the geodesic deviation one obtains for the Liapunov exponent $\omega = \sqrt{\frac{2E}{m}}$. Pesin's equality [9], $h = \omega$, relates ω to the Kolmogorow-Sinai entropy h [10], which in turn determines the exponential proliferation of the closed periodic orbits:

$$\#\{b|T(b) \leq T\} \sim \frac{e^{hT}}{hT} \quad , \quad T \rightarrow \infty \quad ,$$

where b denotes a primitive periodic orbit and $T(b)$ its period. With $l(b) \equiv hT(b)$ = length of periodic orbit b with energy E and period $T(b)$, we obtain Huber's law [11], see Eq.(12) below. Thus the length spectrum $\{l(b)\}$ on M shows an exponential proliferation of long periodic orbits.

II The Length Spectrum of Periodic Orbits

II.1 The Fundamental Domain and the Generating Boosts

Here we briefly describe how to construct a compact Riemann surface of constant negative curvature. The starting point is the whole surface of constant negative curvature called pseudosphere, on which one can define boosts in analogy to translations on the plane. These boosts together with the rotations span the three-dimensional Lorentz group \mathcal{L} on the pseudosphere. Considering a discrete subgroup $G \subset \mathcal{L}$ containing only boosts, one can tessellate the pseudosphere by identifying the points z and z' , where $z' = bz$ and $b \in G$. Figure 1 shows the tessellation of the pseudosphere in regular octagons. The distortion of the octagons near the boundary of the Poincaré disc is due to the metric (1). The tessellation can be viewed as cutting out a piece of the whole pseudosphere and gluing together the edges according to the connection rules of the group G . As already mentioned, we use the Poincaré disc as the model for the pseudosphere. There the Lorentz group is the pseudo-unitary group $SU(1,1)/\{\pm 1\}$, because in the Poincaré disc D a boost or a rotation can be represented by 2×2 matrices

$$T = \begin{pmatrix} \alpha & \beta \\ \beta^* & \alpha^* \end{pmatrix}, \quad |\alpha|^2 - |\beta|^2 = 1, \quad (4)$$

if one defines the action of T on $z \in D$ as the linear fractional transformation

$$z' = Tz := \frac{\alpha z + \beta}{\beta^* z + \alpha^*} \quad (5)$$

The boosts are hyperbolic transformations, i.e. $\frac{1}{2}|\text{Tr}(T)| = |\Re\alpha| > 1$, whereas rotations are elliptic ones, $|\Re\alpha| < 1$. If the subgroup G is generated by the $2g$ generators ($g \geq 2$)

$$b_k = \begin{pmatrix} \cosh \frac{l_0}{2} & e^{i\frac{k\pi}{2g}} \sinh \frac{l_0}{2} \\ e^{-i\frac{k\pi}{2g}} \sinh \frac{l_0}{2} & \cosh \frac{l_0}{2} \end{pmatrix}, \quad k = 0, \dots, 2g - 1, \quad (6)$$

(and their inverses, $k = 2g, \dots, 4g - 1$) where

$$\cosh \frac{l_0}{2} = \cot \frac{\pi}{4g}, \quad (7)$$

the resulting fundamental domain, which has $4g$ edges and an area of $A = 4\pi(g - 1)$, represents a regular surface of genus g .

The $2g$ generators differ only by the factor $e^{i\frac{k\pi}{2g}}$ in the offdiagonal of (6) which determines the direction of the invariant line, defined as the geodesic curve C which is mapped under the action of b_k onto itself. The invariant lines of the b_k 's intersect each other at angles of $\delta = \frac{\pi}{2g}$ at the origin $z = 0$ yielding a regular fundamental domain. Eq.(7) follows from elementary hyperbolic geometry: The dotted triangle in Fig. 1 has an area

$$A_{\Delta} = \frac{A}{8g} = \frac{4\pi(g - 1)}{8g} = \pi - (\alpha + \beta + \gamma),$$

and from $\alpha = \frac{\delta}{2} = \frac{\pi}{4g}$ and $\gamma = \frac{\pi}{2}$ one obtains $\beta = \frac{\pi}{4g} = \alpha$. Furthermore (see Fig. 1)

$$\cosh b = \frac{\cos \beta}{\sin \alpha} = \cot \alpha = \cot \frac{\pi}{4g},$$

and realizing that b_k translates a point z by the distance $l_0 = 2b$, one arrives at Eq.(7).

II.2 The Periodic Orbits

Now we describe our method to find all periodic orbits, at least theoretically. In practice this method yields the lower part of the length spectrum which is most important in using the Selberg trace formula.

Every group element $b \in G$ belongs to a periodic orbit. Hence one can find the length spectrum by calculating all group elements by forming the product out of the generating boosts b_k and their inverses

$$b = b_{i_1} b_{i_2} \dots b_{i_n} = \begin{pmatrix} \alpha & \beta \\ \beta^* & \alpha^* \end{pmatrix} . \quad (8)$$

The length $l(b)$ of the periodic orbit belonging to this $b \in G$ depends only on the real part of α

$$l(b) = 2 \operatorname{arccosh} |\Re \alpha| . \quad (9)$$

To confirm Eq.(9), consider the eigenvalues of the matrix b_k which represents the corresponding generator:

$$\det \begin{vmatrix} \cosh \frac{l_0}{2} - \lambda & e^{i \frac{k\pi}{2g}} \sinh \frac{l_0}{2} \\ e^{-i \frac{k\pi}{2g}} \sinh \frac{l_0}{2} & \cosh \frac{l_0}{2} - \lambda \end{vmatrix} = \lambda^2 - 2\lambda \cosh \frac{l_0}{2} + 1 = 0$$

$$\lambda_{1,2} = \cosh \frac{l_0}{2} \pm \sqrt{\cosh^2 \frac{l_0}{2} - 1} . \quad (10)$$

The eigenvalues are fixed by the length l_0 of the periodic orbit. Repeating the same procedure for an arbitrary boost $b \in G$ as given by Eq.(8), one obtains for the eigenvalues $\lambda_{1,2} = \Re \alpha \pm \sqrt{(\Re \alpha)^2 - 1}$. Since G is a subgroup of the quotient group $SU(1,1)/\{\pm 1\}$, one must take $|\Re \alpha|$ instead of $\Re \alpha$, which then gives Eq.(9).

However, if one would generate all group elements successively one would count the orbits repeatedly because two group elements b and \bar{b} have the same orbit if they belong to the same conjugacy class $[b] = \{b' | b' = \hat{b} b \hat{b}^{-1}, \hat{b} \in G\}$. In other words, one must generate the conjugacy classes instead of the group elements itself. In addition, there is the identity

$$b_0 b_1^{-1} b_2 b_3^{-1} b_0^{-1} b_1 b_2^{-1} b_3 = 1 ,$$

which has to be used in its many equivalent forms in the process of enumerating the conjugacy classes. Therefore we developed a computer program which successively generated the conjugacy classes for the surface of genus $g = 2$ corresponding to the regular octagon shown in Fig.1. It calculated all conjugacy classes which had elements consisting of a product up to 9 generating boosts b_k . This program provided more than 2.6 million conjugacy classes to which belong more than 21,000 orbits of different lengths. The first 80 different lengths of primitive orbits are given in Table 1. The Table shows that many orbits have the same length which is denoted as multiplicity. This multiplicity is expected to be a bit too low at greater lengths because our computation takes only into account the conjugacy classes consisting of products of at most 9 generating boosts. Products of ten and more generating boosts may contribute to the length spectrum at length of order 11 or larger. The column "multiplicity" in Table 1 sometimes contains a number in parenthesis which must be added to the multiplicity if one is interested in the multiplicity of all orbits including multiple traversals, i.e. non primitive orbits. The integers m and n are explained in Sect. II.4 below.

Some periodic orbits are shown as an illustration in their fundamental domains in Figure 2. Figures 2a to 2f display orbits in the regular octagon, whereas Figures 2g and 2h represent examples in the case of surfaces of genus $g = 3$ and $g = 8$ respectively.

length of periodic orbit	multiplicity	m	n	length of periodic orbit	multiplicity	m	n
3.0571418390	24	1	1	10.8758208811	96	57	41
4.8969048954	24	3	2	10.9343449467	256	59	42
5.8280707754	48	5	3	10.9912049969	432	61	43
6.1142836779	0 (24)	5	4	11.0464930504	96	63	44
6.6720057699	96	7	5	11.0689538604	288	63	45
7.1073758741	48	9	6	11.1221615882	192	65	46
7.2631634751	48	9	7	11.1739903506	384	67	47
7.5956918304	8	11	8	11.2450675676	544	69	49
7.8806922887	96	13	9	11.2938444648	272	71	50
8.1300755289	48	15	10	11.3414600077	272	73	51
8.2249036233	192	15	11	11.3608557221	96	73	52
8.4368496405	48	17	12	11.4069202001	672	75	53
8.6284636565	96	19	13	11.4519475300	192	77	54
8.7027505564	48	19	14	11.4703055581	464	77	55
8.8714798107	288	21	15	11.5139434106	48	79	56
9.0270717197	12	23	16	11.5566494092	648	81	57
9.1714255169	48 (24)	25	17	11.5984625221	40	83	58
9.2282950896	96	25	18	11.6155292590	544	83	59
9.3592716579	192	27	19	11.6561415509	192 (48)	85	60
9.4821941493	48	29	20	11.6959455360	416	87	61
9.5309770571	192	29	21	11.7122036393	288	87	62
9.6440656486	96	31	22	11.7509179318	496	89	63
9.7510997583	336	33	23	11.7888970234	96	91	64
9.7938097907	4 (24)	33	24	11.8044196553	192	91	65
9.8933106878	192	35	25	11.8414054395	352	93	66
9.9880946367	192	37	26	11.8777196407	544	95	67
10.0785887303	192	39	27	11.9133862138	24	97	68
10.1149054114	96	39	28	11.9279754971	512	97	69
10.1999558888	384	41	29	11.9627646508	352	99	70
10.2815363765	96	43	30	11.9969589861	384	101	71
10.3143770353	192	43	31	12.0443403136	544	103	73
10.3915072941	32	45	32	12.0771791386	288	105	74
10.4657729697	384	47	33	12.1094874621	352	107	75
10.5373792543	96	49	34	12.1227186314	96	107	76
10.5663046423	288	49	35	12.1543053200	800	109	77
10.6344594911	96	51	36	12.1854008904	352	111	78
10.7003680283	272	53	37	12.1981408207	368	111	79
10.7270445783	96	53	38	12.2285673558	48 (24)	113	80
10.7900178989	560	55	39	12.2585379275	736	115	81
10.8510687003	40	57	40	12.2708217905	96	115	82

Table 1: The first 80 lengths of the length spectrum of the regular octagon

II.3 The asymptotic behaviour of the length spectrum

Let us define the number $N(l)$ of all primitive orbits of length less than l by

$$N(l) := \sum_{l_n \leq l} g_n \quad (11)$$

where the g_n 's are the multiplicities of the lengths l_n which are ordered as $0 < l_0 < l_1 < l_2 < \dots$. The periodic orbits proliferate exponentially for long lengths as shown by Huber [11]

$$N(l) \sim \frac{e^l}{l} \left(\sum_{n=0}^N \frac{n!}{l^n} + O(l^{-N-1}) \right) , \quad l \rightarrow \infty . \quad (12)$$

This behaviour is characteristic for chaotic systems, whereas a power-law determines the proliferation of periodic orbits in the case of integrable systems. The asymptotic expression (12) coincides well with our computation down to the shortest lengths as depicted in Fig. 3, where we take into account the correction terms up to $N = 3$. Above $l \simeq 12$ the calculated staircase function is below the prediction (12), see the dotted line in Fig.3, which is a reflection of missing lengths as explained in Sect.II.2. With the aid of our computation we have empirically found the law which determines the proliferation of the different lengths themselves

$$\hat{N}(l) := \sum_{l_n \leq l} 1 \quad (13)$$

without regard to their multiplicities. The law

$$\hat{N}(l) \sim \frac{2}{\rho} e^{\frac{l}{2}} , \quad l \rightarrow \infty , \quad (14)$$

with $\rho = 11.3$ is in excellent agreement with our numerical results. In order to check Eq.(14), consider the length differences between two adjacent lengths ("length density")

$$\frac{1}{l_{n+1} - l_n} = \frac{\Delta \hat{N}}{\Delta l} \sim \frac{d\hat{N}(l_n)}{dl} \sim \frac{1}{\rho} e^{\frac{l_n}{2}} \quad (15)$$

and define

$$\delta(n) := (l_{n+1} - l_n) \frac{e^{\frac{l_n}{2}}}{\rho} \quad (16)$$

which should fluctuate around 1 if Eq.(14) is correct. Indeed this behaviour is confirmed in Fig. 4, where we use $\rho = 8\sqrt{2}$ as will be explained later. The exceptionally high spikes seen in Fig. 4 are almost certainly due to missing orbits which are generated by more than 9 boosts. The law (14) uniquely determines the mean multiplicity $\hat{g}(l)$: To be consistent with Huber's law, the following asymptotic law should hold

$$\hat{g}(l) \sim \rho \frac{e^{\frac{l}{2}}}{l} . \quad (17)$$

Figure 5 reveals large fluctuations around this mean multiplicity $\hat{g}(l)$. If one compares, however, the mean value \bar{g}_n over the intervall $[l_n - \frac{1}{2}, l_n + \frac{1}{2}]$

$$\bar{g}_n = \frac{1}{N} \sum_{l_n - \frac{1}{2} < l_k < l_n + \frac{1}{2}} g_k \quad (18)$$

with the mean multiplicity $\hat{g}(l)$, one observes good agreement until lengths of order 11 or 12 (Fig. 6). Above these lengths the mean multiplicity \bar{g}_n lies somewhat below $\hat{g}(l)$ for reasons explained above.

II.4 Arithmetical Properties of Periodic Orbits

Each boost

$$b = \begin{pmatrix} \alpha & \beta \\ \beta^* & \alpha^* \end{pmatrix} \in G$$

can be represented in the case of genus $g = 2$ by algebraic numbers (here the algebraic numbers are of the form $n_1 + \sqrt{2}n_2$, $n_1, n_2 \in \mathbf{N}$) :

$$\alpha = n_1 + \sqrt{2}n_2 + i(n_3 + \sqrt{2}n_4) = a + \sqrt{2}b \quad , \quad (19)$$

where $n_i \in \mathbf{N}$ and $a = n_1 + in_3$, $b = n_2 + in_4$. The offdiagonal element β has the form $\beta = \sqrt{1 + \sqrt{2}(c + \sqrt{2}d)}$ where c and d are of the same form as a and b but with $n_i \in \mathbf{Z}$. Indeed, any boost $b \in G$ has the representation

$$b = \begin{pmatrix} a + \sqrt{2}b & \sqrt{1 + \sqrt{2}(c + \sqrt{2}d)} \\ \sqrt{1 + \sqrt{2}(c^* + \sqrt{2}d^*)} & a^* + \sqrt{2}b^* \end{pmatrix} \quad , \quad (20)$$

because on the one hand the generating boosts b_k have this form as follows from Eqs.(6) and (7) for genus $g = 2$ combined with

$$\cosh \frac{l_0}{2} = \cot \frac{\pi}{8} = 1 + \sqrt{2} \quad , \quad (21)$$

and on the other hand every product of matrices of the form (20) is again a matrix of this form :

$$\begin{aligned} b\hat{b} &= \begin{pmatrix} a + \sqrt{2}b & \sqrt{1 + \sqrt{2}(c + \sqrt{2}d)} \\ \sqrt{1 + \sqrt{2}(c^* + \sqrt{2}d^*)} & a^* + \sqrt{2}b^* \end{pmatrix} \begin{pmatrix} \hat{a} + \sqrt{2}\hat{b} & \sqrt{1 + \sqrt{2}(\hat{c} + \sqrt{2}\hat{d})} \\ \sqrt{1 + \sqrt{2}(\hat{c}^* + \sqrt{2}\hat{d}^*)} & \hat{a}^* + \sqrt{2}\hat{b}^* \end{pmatrix} \\ &= \begin{pmatrix} \alpha & \beta \\ \beta^* & \alpha^* \end{pmatrix} \end{aligned} \quad (22)$$

where

$$\alpha = (a + \sqrt{2}b)(\hat{a} + \sqrt{2}\hat{b}) + (1 + \sqrt{2})(c + \sqrt{2}d)(\hat{c} + \sqrt{2}\hat{d}) = a' + \sqrt{2}b' \quad (23)$$

$$\beta = \sqrt{1 + \sqrt{2}} \left[(a + \sqrt{2}b)(\hat{c} + \sqrt{2}\hat{d}) + (c + \sqrt{2}d)(\hat{a} + \sqrt{2}\hat{b}) \right] = \sqrt{1 + \sqrt{2}}(c' + \sqrt{2}d') \quad (24)$$

and a', b', c', d' are again of the form $n'_1 + in'_2$. Thus each orbit length is simply determined by $|\Re\alpha| = m + \sqrt{2}n$, $m, n \in \mathbf{N}$, and because of this important fact these two integers are given in Table 1 too. There one makes a surprising discovery: The n 's are running through all natural numbers with two exceptions, because there are no orbits at $n = 48$ and $n = 72$. These voids are probably filled up if one takes into account conjugacy classes with elements consisting of ten and more generating boosts. The rule for the integers m is not so simple. They run through all odd integers but there are sometimes "pairs" of odd integers without any systematics, as it appears at first sight. Nevertheless one can reproduce the sequence (m, n) by the following " $\sqrt{2}$ -rule":

- $n = 1, 2, 3, \dots$
- m is that odd natural number which minimizes $|\frac{m}{n} - \sqrt{2}|$.

So the sequence (m, n) is simply a sequence which approximates $\sqrt{2}$ supplemented by the subsidiary condition that m is an odd natural number. Therefore the length spectrum is completely determined by its arithmetical properties, see Eq.(26) below. Unfortunately we are unable to formulate a likewise simple rule for the multiplicity.

We would like to mention a connection between the “pairs” in the m sequence and the so-called Beatty sequence. The “pairs” of m occur at the following values of n :

$$3, 6, 10, 13, 17, 20, 23, 27, 30, \dots \quad (25)$$

The same sequence appears in a special case of Beatty’s theorem [12] which states:

If $\frac{1}{x} + \frac{1}{y} = 1$, where x and y are positive irrational numbers, then the sequences

$$[x], [2x], [3x], \dots \quad [y], [2y], [3y], \dots$$

together include every positive integer just once, where $[x]$ means the integral part of x .

By the special choice $x = 2 + \sqrt{2}$ and $y = \sqrt{2}$ the sequence $[x], [2x], [3x], \dots$ is exactly the sequence (25).

Let us now show that the law (14) follows from the “ $\sqrt{2}$ -rule”. Writing Eq.(19) in the form

$$\cosh \frac{l_n}{2} = m + \sqrt{2}n \quad , \quad m, n \in \mathbf{N} \quad (26)$$

we could use $m = \lceil \sqrt{2}n \rceil$. But to get a more manageable expression we instead use the asymptotically correct value $m = \sqrt{2}n$ despite of the fact that this m is not an integer of course. Then we can asymptotically express Eq.(26) as

$$\frac{1}{2}e^{\frac{l_n}{2}} \sim 2\sqrt{2}n \quad (27)$$

or

$$n \sim \frac{1}{4\sqrt{2}}e^{\frac{l_n}{2}} \quad (28)$$

Realizing that l_n is the n th length we have recovered Eq.(14) :

$$\hat{N}(l) \sim \frac{2}{8\sqrt{2}}e^{\frac{l}{2}} \quad , \quad \text{whence } \rho = 8\sqrt{2} \quad (29)$$

The theoretical value $\rho = 8\sqrt{2} = 11.31\dots$ is in excellent agreement with our empirical value 11.3 determined from Fig. 4.

III Summary and Discussion

In this paper we have presented for the first time an explicit enumeration of the shortest periodic orbits (classical paths) for a prototype example of a chaotic Hamiltonian system: a point particle sliding freely on a two-dimensional surface of constant negative curvature. Our computations crucially relied on the intimate relation between the periodic orbits and the topology, geometry and group theory of compact Riemann surfaces of genus $g \geq 2$. To keep things as simple as possible, we have chosen $g = 2$ and considered the most regular fundamental region, i.e. the hyperbolic octagon shown in Fig. 1. The corresponding Riemann surface M can be identified with D/G , the action of a particular Fuchsian group, the “octagon group” G on the Poincaré disc D . The octagon group G can be constructed from 8 generators b_k ($k = 0, 1, \dots, 7$) playing the role of boosts, whose explicit matrix representation has been given in Eq.(6). By forming all possible “words” of arbitrary length from the alphabet consisting

of the 8 “letters” b_k by matrix multiplication, one can construct in principle all group elements of G . Of great importance is the classification of the group elements in terms of conjugacy classes, since such a classification is equivalent to an enumeration of periodic orbits on M . The (hyperbolic) length $l(b)$ of a periodic orbit corresponding to a given group element $b \in G$ is uniquely determined by Eq.(9). Although one is led along these lines to a well defined algorithm for calculating the periodic orbits together with their lengths, the actual computation could only be carried out on a large computer. Within the computer time available to us, we were able to reconstruct all words with a maximal length of 9 letters. As a result we obtained 2,605,593 primitive periodic orbits. The shortest 80 lengths and their multiplicities have been given in Table 1. A few typical examples of periodic orbits have been displayed in Figs. 2a–h. Surprisingly enough, the “length staircase” $N(l)$, defined in Eq.(11), is nicely described by the asymptotic behaviour (12) down to the shortest lengths, as can be seen from Fig.3. Only at the upper end of the staircase one observes a deviation, which is caused by missing words formed out of 10 or more letters.

In Sect. II.4 we derived a curious representation of the group elements $b \in G$, Eq.(20), in terms of algebraic numbers of the form $n_1 + \sqrt{2}n_2$, $n_i \in \mathbf{Z}$. Thus the length spectrum $\{l(b)\}$ is completely determined by its arithmetical properties as given in Eq.(26). We have thus discovered a close connection between the length spectrum of the octagon group G and number theory. It is hoped, that this connection can be deepened in order to shed some light on the multiplicity distribution and to reveal the arithmetical structure of chaos. Work in this direction is being carried out. Using the arithmetic properties of the length spectrum we could derive the asymptotic law (14) and thus predict the value $8\sqrt{2}$ for the parameter ρ which, originally, was introduced as a free parameter in Eq.(14). The predicted value for ρ is in excellent agreement with our numerical results (see Figs. 4–6) which gave $\rho = 11.3$.

The length spectrum obtained in this paper constitutes an important input in the Selberg trace formula [3–6], which is an exact substitute for the Bohr–Sommerfeld–Einstein quantization rules for our chaotic system, and which can be interpreted as an (exact) instanton–gas evaluation of the corresponding Feynman path integral. It establishes a striking duality relation between the quantum mechanical energy spectrum and the lengths of the classical trajectories. On the basis of this exact “periodic orbit theory” we hope to unravel the mystery of quantum chaos. Investigations along these lines are under study and will be published elsewhere.

Acknowledgement

We would like to thank G.Münster for drawing our attention to [12].

References

- [1] N.L.Balazs and A.Voros , Physics Reports 143(1986) 109
- [2] See e.g. M.V.Berry , Proc. R. Soc. Lond. A400(1985) 229 ; ibid. A413(1987) 183
- [3] M.C.Gutzwiller , Phys. Rev. Lett. 45(1980) 150 ; Physica Scripta T9(1985) 184
- [4] A.Selberg , J. Indian Math. Soc. 20(1956) 47
- [5] F.Steiner , Physics Letters B 188(1987) 447
- [6] F.Steiner , DESY Preprint 87 - 022 and Proceedings of the Schladming Conference 1987
- [7] E.Artin , Abh. Math. Sem. Universität Hamburg 3(1924) 170
- [8] D.V.Anosov , Proc Steklov Inst. of Math. 90(1967) , Am. Math. Soc. Trans. 1969
- [9] Ya.V.Pesin , Sov. Math. Dokl. 17(1976) 196
- [10] See e.g. Ya.G. Sinai , Introduction to Ergodic Theory (Princeton University Press , 1976)
- [11] H.Huber , Math. Annalen 138(1959) 1
- [12] H.S.M. Coxeter , Scripta Mathematica 19(1953) 135 ;
I.G.Connell , Can. Math. Bulletin 2(1959) 181 , 190 ; ibid. 3(1960) 17

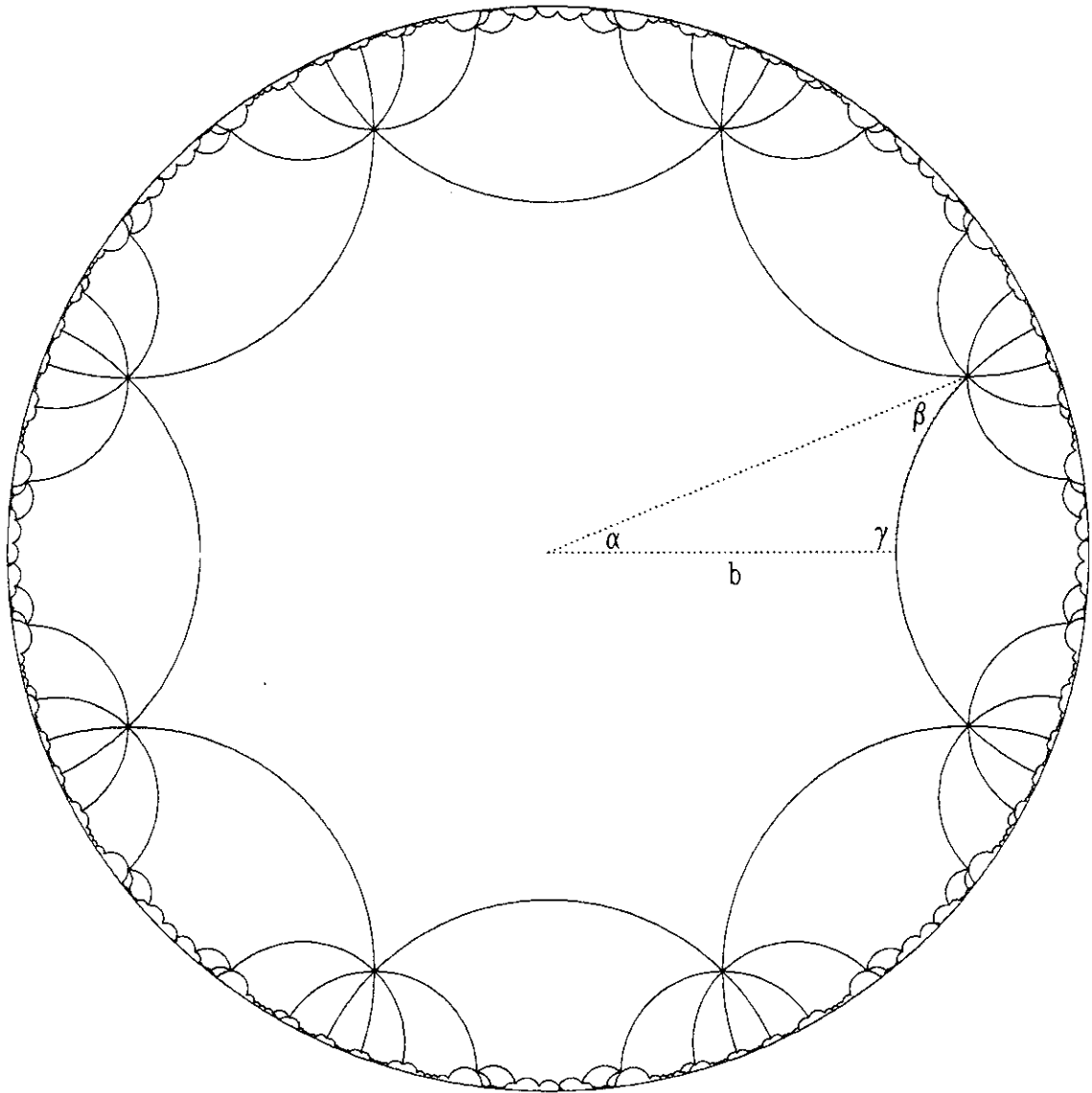


Fig. 1 : The tessellation of the pseudosphere in regular octagons.

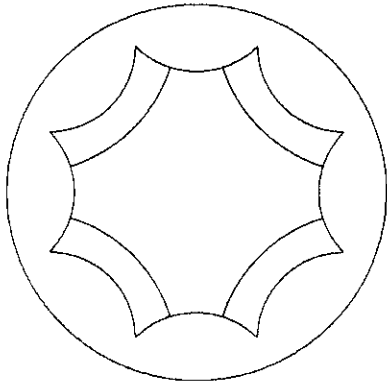


Fig 2a : The periodic orbit in the regular octagon belonging to $b_0 b_2 b_0^{-1} b_2^{-1}$
 $(m,n) = (23,16)$; $l_n = 9.02707\dots$

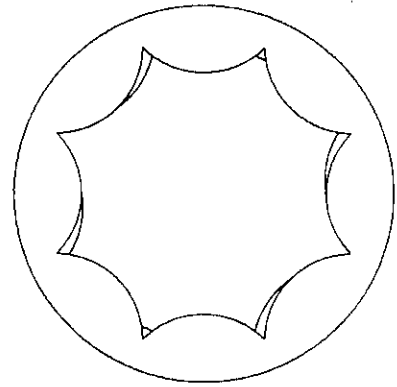


Fig. 2b : The periodic orbit in the regular octagon belonging to $b_0 b_1^{-1} b_2 b_3^{-1} b_2 b_1^{-1}$
 $(m,n) = (5,3)$; $l_n = 5.82807\dots$

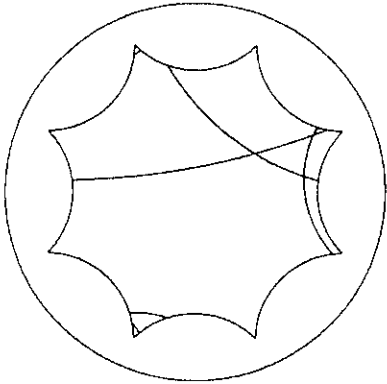


Fig 2c : The periodic orbit in the regular octagon belonging to $b_0 b_1 b_2^{-1} b_3 b_1 b_2^{-1}$
 $(m,n) = (39,27)$; $l_n = 10.07858\dots$

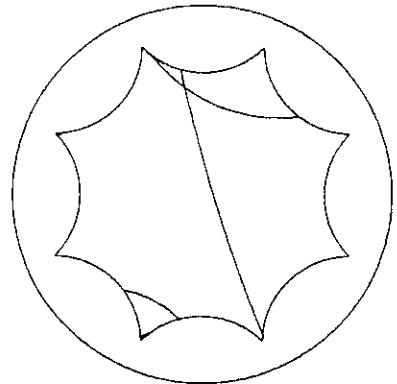


Fig. 2d : The periodic orbit in the regular octagon belonging to $b_0 b_3 b_2 b_1^{-1} b_2 b_1^{-1}$
 $(m,n) = (15,11)$; $l_n = 8.22490\dots$

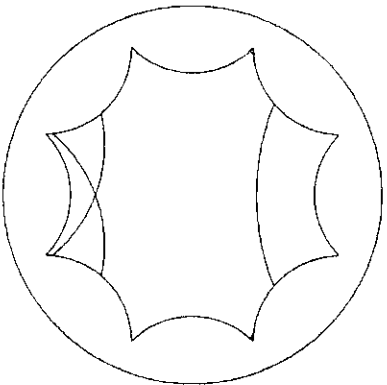


Fig 2e : The periodic orbit in the regular octagon belonging to $b_1 b_3 b_1 b_3 b_2^{-1}$
 $(m,n) = (15,11)$; $l_n = 8.22490\dots$

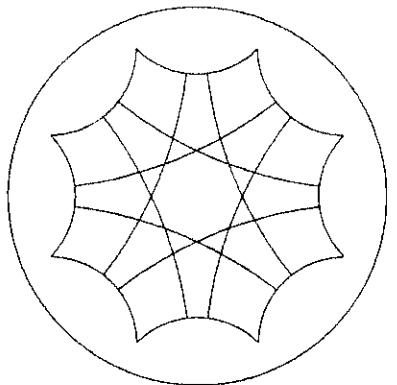


Fig. 2f : The periodic orbit in the regular octagon belonging to $b_0 b_1 b_2 b_3 b_0^{-1} b_1^{-1} b_2^{-1} b_3^{-1}$
 $(m,n) = (25343,17920)$; $l_n = 23.05309\dots$

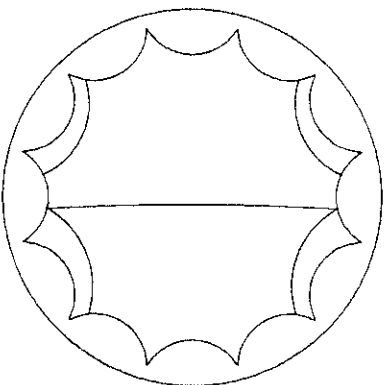


Fig. 2g : The periodic orbit in the case of genus $g=3$ belonging to $b_0 b_0 b_3 b_0 b_3$

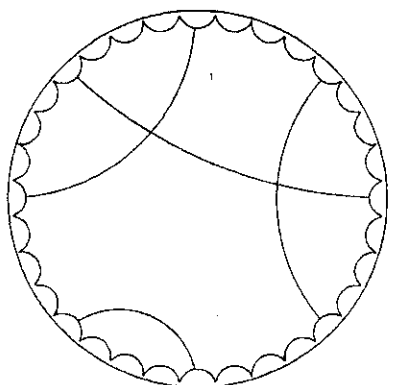
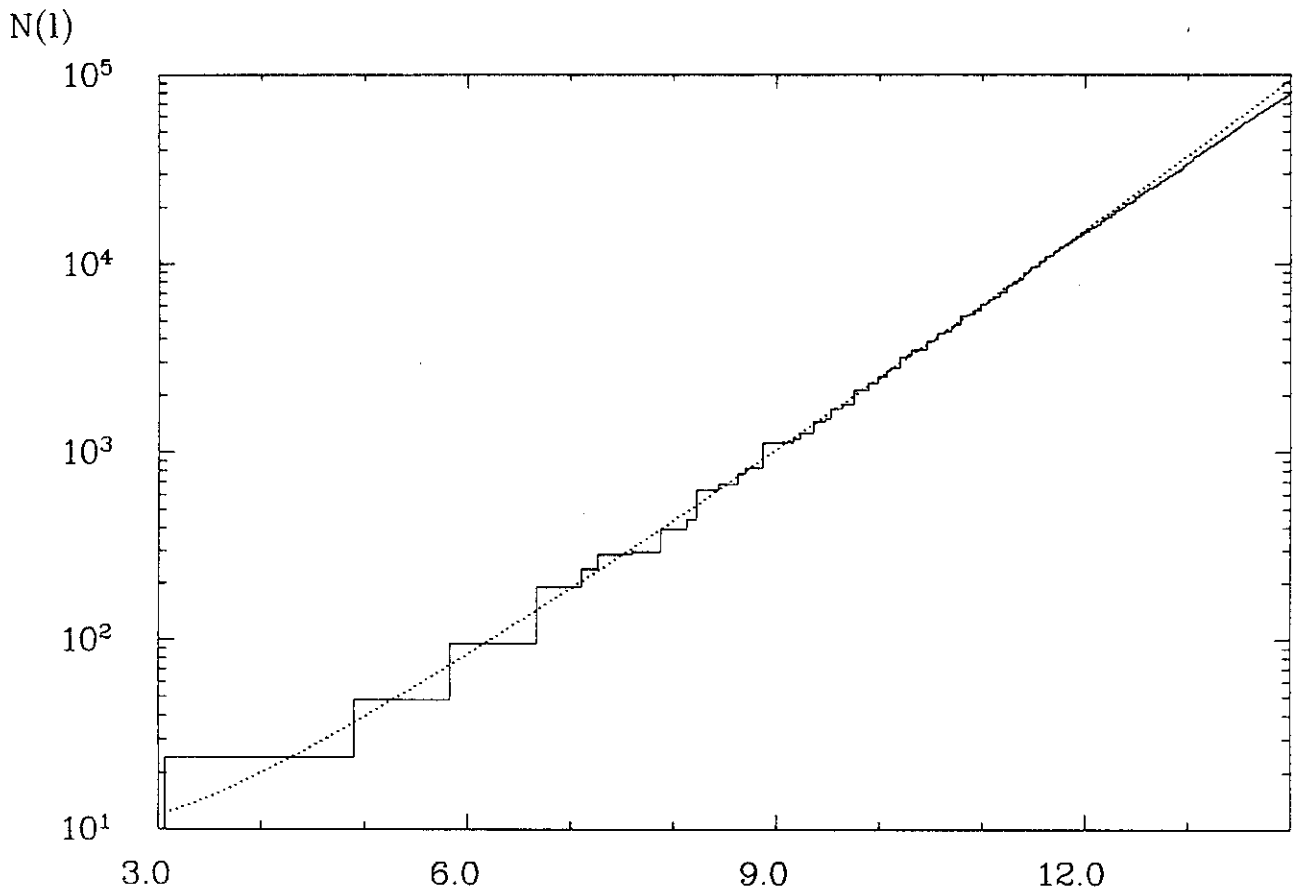


Fig. 2h : The periodic orbit in the case of genus $g=8$ belonging to $b_0 b_2 b_3 b_7$



1

Fig. 3 : The staircase function $N(l)$ as defined in eq.(11) in comparison with Huber's law (12) (dotted line) .

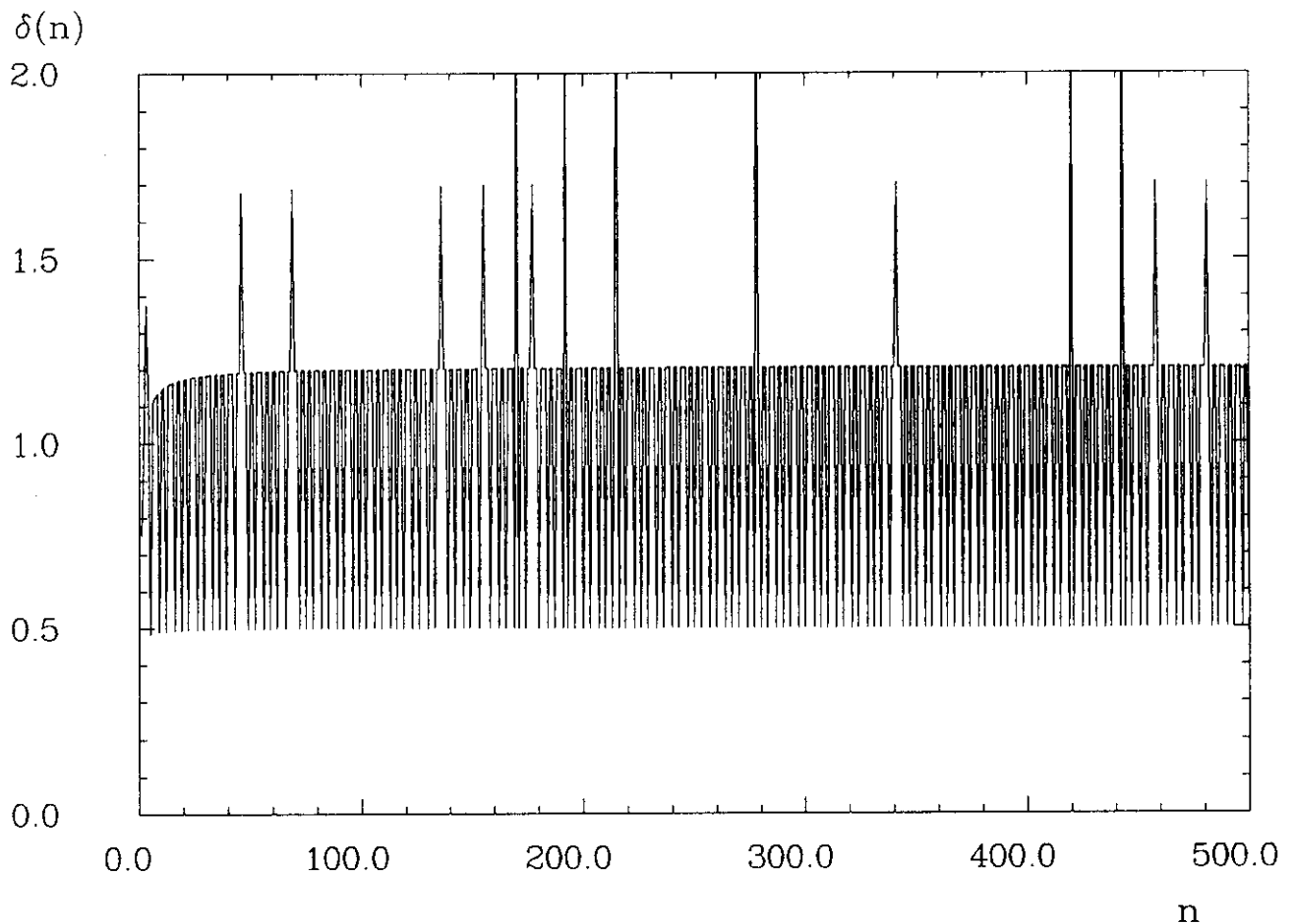


Fig. 4 : The length differences weighted by $\exp(l_n/2)/\rho$ are shown where $\rho = 8\sqrt{2}$.

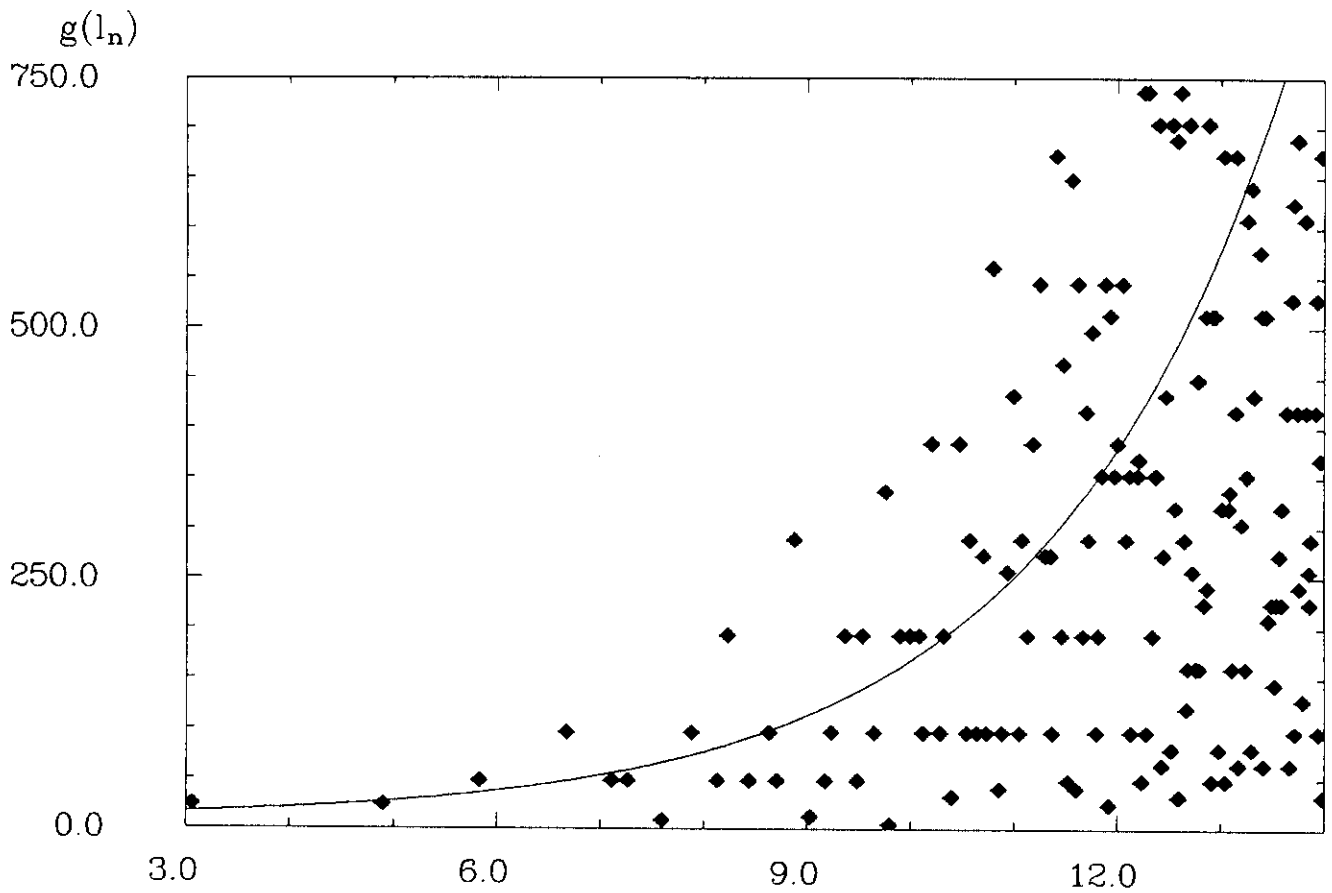


Fig. 5 : The multiplicity g_n of the orbit length l_n plotted as squares is compared with the mean multiplicity (17) (the smooth curve) .

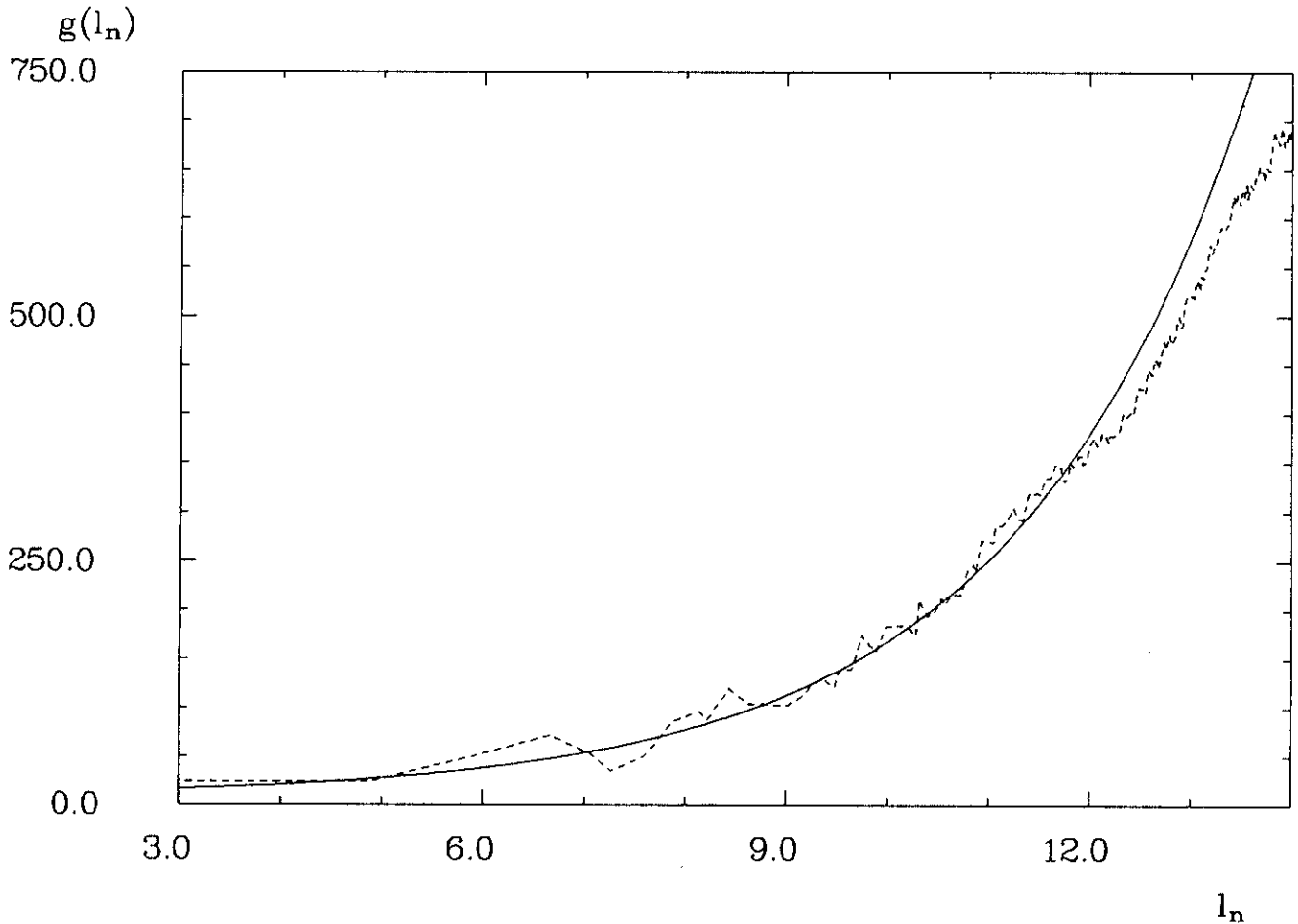


Fig. 6 : The mean multiplicity (18) is plotted as dashed line and is compared with $\hat{g}(l)$ eq.(17) (the smooth curve) .